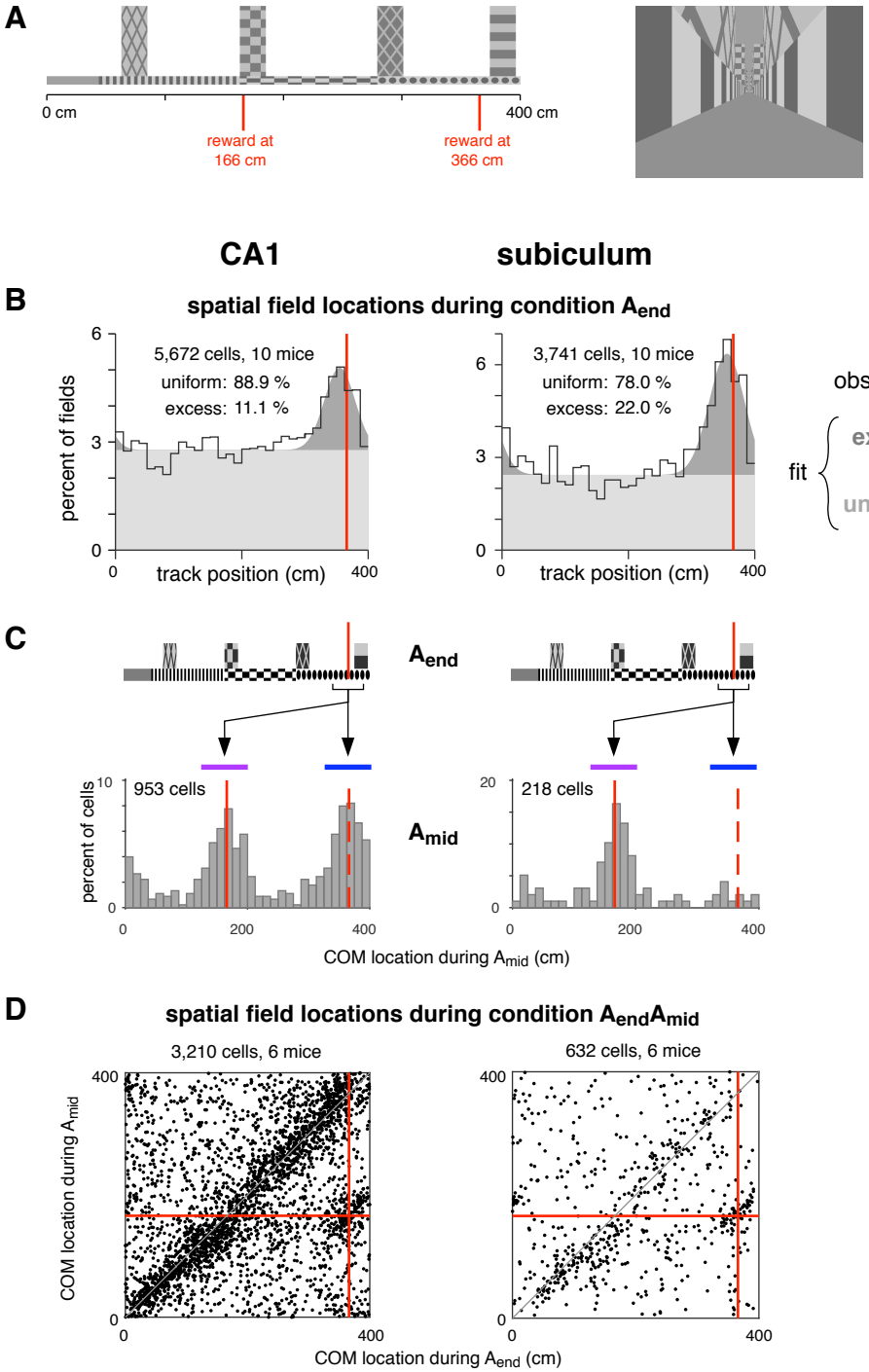
A
0 cm
400 cm
reward at
166 cm
reward at
366 cm
CA1
subiculum
B
spatial field locations during condition A_{end}
5,672 cells, 10 mice
uniform: 88.9 %
excess: 11.1 %
3,741 cells, 10 mice
uniform: 78.0 %
excess: 22.0 %
percent of fields
track position (cm)
observed
fit
excess
uniform
C
A_{end}
A_{mid}
953 cells
218 cells
percent of cells
COM location during A_{mid} (cm)
D
spatial field locations during condition $A_{end}A_{mid}$
3,210 cells, 6 mice
632 cells, 6 mice
COM location during A_{mid}
COM location during A_{end} (cm)

Figure S1. Reward-associated cells were found in both CA1 and subiculum in condition $\mathbf{A_{end}A_{mid}}$, Related to Figure 1.
(A) Scale diagram of track A in side view (left) and perspective rendering from inside the track (right).
(B-D) Analyses were performed separately for CA1 (left panels) and subiculum (right panels).
(B) Density of spatial field COMs. Black line shows observed density, gray patches show density of a fitted mixture distribution consisting of a uniform distribution (light gray) and a Gaussian distribution (dark gray, mean 355 cm, s.d. 24 cm for CA1, mean 356 cm, s.d. 28 cm for subiculum).
(C) COM location during A_{mid} for cells with a COM located within 25 cm (before or after) reward during A_{end}. Same graphical conventions as in Figure 1F. Although very few place cells in the subiculum were located near 366 cm, there was still a population of reward-associated cells whose fields remapped to be consistently active near reward.
(D) COM locations of cells with a spatial field during both A_{end} and A_{mid}. Same graphical conventions as in Figure 1G.

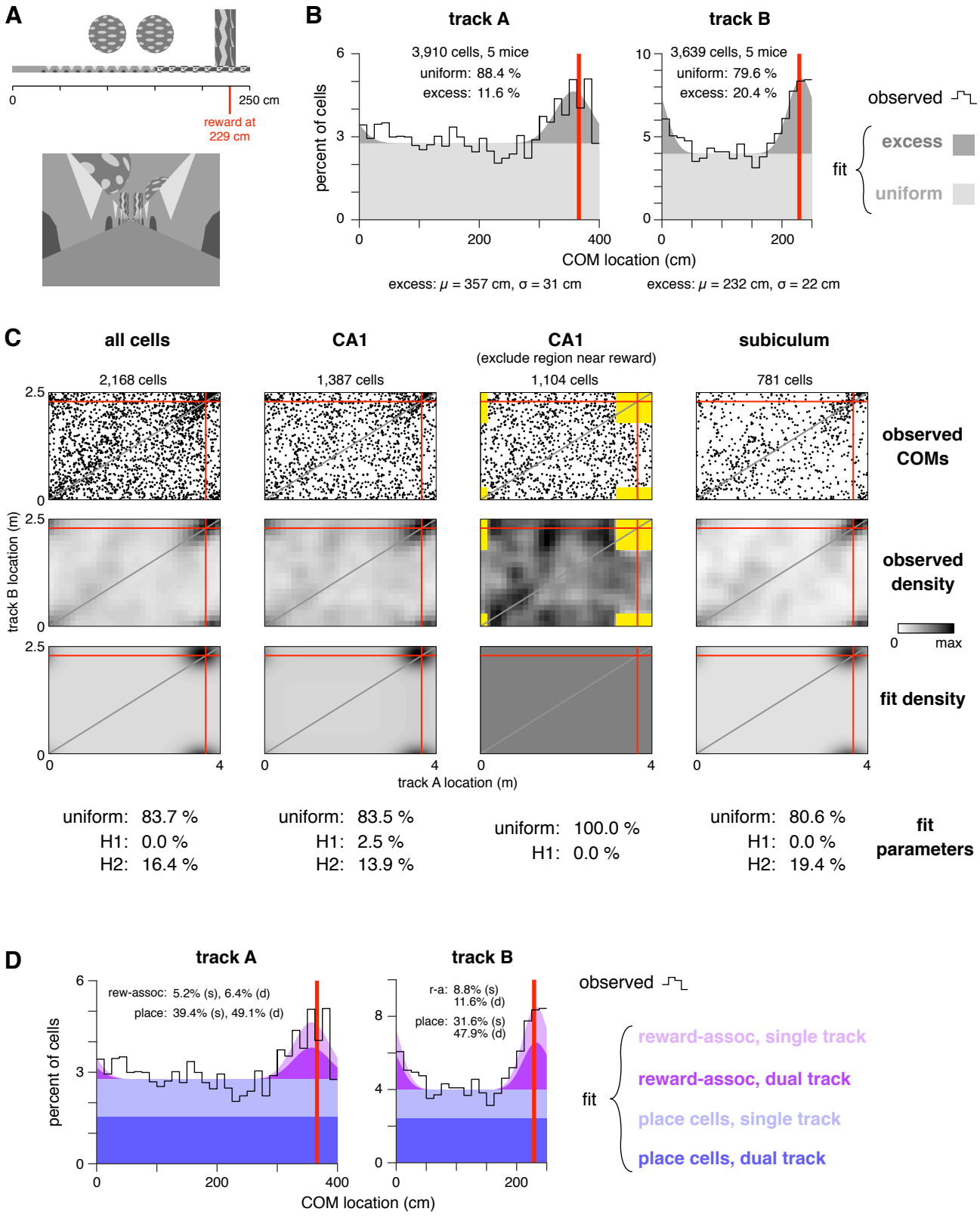
A
0
250 cm
reward at
229 cm
B
track A
track B
3,910 cells, 5 mice
uniform: 88.4 %
excess: 11.6 %
3,639 cells, 5 mice
uniform: 79.6 %
excess: 20.4 %
percent of cells
COM location (cm)
observed
fit
excess
uniform
excess: μ = 357 cm, σ = 31 cm
excess: μ = 232 cm, σ = 22 cm
C
all cells
CA1
CA1
(exclude region near reward)
subiculum
2,168 cells
1,387 cells
1,104 cells
781 cells
observed
COMs
observed
density
0
max
fit density
track B location (m)
track A location (m)
uniform: 83.7 %
H1: 0.0 %
H2: 16.4 %
uniform: 83.5 %
H1: 2.5 %
H2: 13.9 %
uniform: 100.0 %
H1: 0.0 %
uniform: 80.6 %
H1: 0.0 %
H2: 19.4 %
fit
parameters
D
track A
track B
rew-assoc: 5.2% (s), 6.4% (d)
place: 39.4% (s), 49.1% (d)
r-a: 8.8% (s)
11.6% (d)
place: 31.6% (s)
47.9% (d)
percent of cells
COM location (cm)
observed
fit
reward-assoc, single track
reward-assoc, dual track
place cells, single track
place cells, dual track

Figure S2. Analysis of COM density in condition AB, Related to Figure 2.
(A) Scale diagram of track B in side view (top) and perspective rendering from inside the track (bottom). (B-D) Red lines indicate reward location.
(B) During condition AB, COMs were located at excess density near reward on both track A (left) and track B (right). Black outlines show observed COM density, and solid patches show fit density of uniform distribution (light gray) and the excess density near reward modeled as a Gaussian (dark gray). Inset numbers show fit coefficients of the mixture distribution. Numbers at bottom show parameters of Gaussian fit.
(C) Among cells with a spatial field on both tracks, the excess density was entirely explained by H2 rather than H1 (see Results and STAR Methods). Each column shows analysis of COMs from a different cell group. First row: observed COM locations. Second row: observed COM density, binned in 12.5 cm bins, smoothed with a Gaussian kernel (15 cm radius). Third row: Density of fit mixture distribution. Fourth row: fit coefficients of mixture distribution. The fit to all CA1 neurons (second column) seemed to indicate some cells remapped according to H1 (2.5%). However, this was an artifact caused by the density near the reward being poorly fit by a Gaussian. After excluding the region within 50 cm of both rewards (yellow patches in third column), there was no contribution from H1 (0.0%). Since the two hypothesis made nearly identical predictions about COM density in this region, excluding it did not bias the fit.
(D) The observed distribution of COM locations (black outline) was modeled as a collection of place cells and reward-associated cells (colored patches) based on the results of the H1-H2 fits (see STAR Methods). The excess COM density near reward was entirely composed of reward-associated cells. The fitted model was further decomposed into populations of cells with a spatial field on one track or on both tracks.

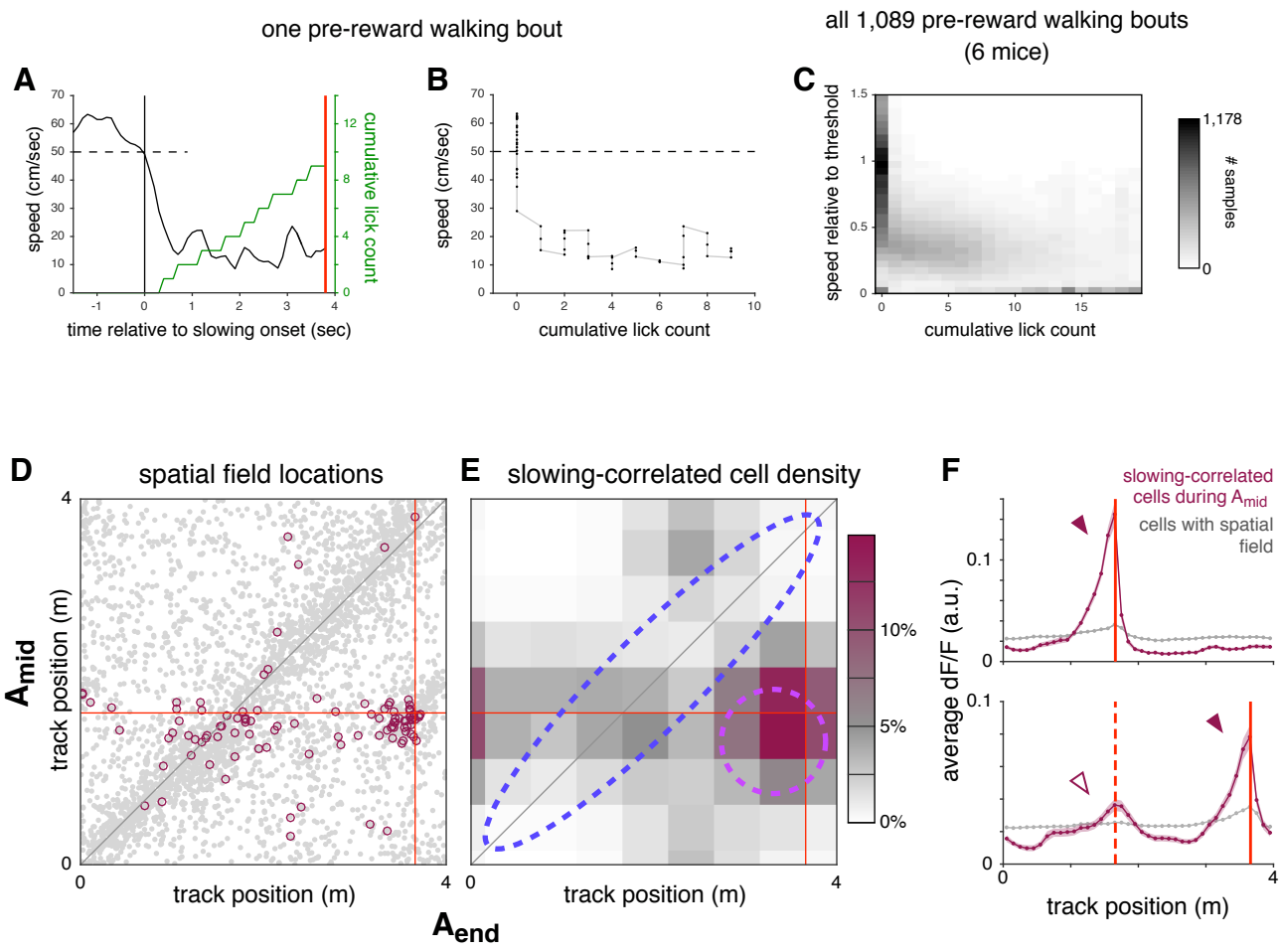
one pre-reward walking bout
all 1,089 pre-reward walking bouts
(6 mice)
A
B
C
speed (cm/sec)
cumulative lick count
time relative to slowing onset (sec)
cumulative lick count
speed relative to threshold
cumulative lick count
1,178
samples
0
D
spatial field locations
E
slowing-correlated cell density
F
track position (m)
track position (m)
10%
5%
0%
slowing-correlated cells during A_mid
cells with spatial field
average dF/F (a.u.)
track position (m)
A_mid
A_end

Figure S3. Slowing preceded licking during reward approach, and most slowing-correlated cells were reward-predictive cells during context A_{mid}, Related to Figure 3.
(A) Speed (black) and cumulative lick rate (green) sampled at 10 Hz for a representative pre-reward walking bout. Dashed line indicates speed threshold. Red line indicates reward delivery.
(B) Scatter plot of speed vs cumulative lick rate (same data as panel A).
(C) Density of speed vs cumulative lick rate for all pre-reward walking bouts with at least 5 licks during condition $A_{end}A_{mid}$. Values were collected in the time interval from 2 seconds prior to slowing until reward delivery. In nearly every case, speed was significantly reduced prior to the first lick, showing that slowing preceded licking.
(D-F) Same analysis as main Figure 3I,J applied to cells that were slowing-correlated during blocks of context A_{mid}.
(D) COM locations of cells with spatially-modulated fields in both A_{end} and A_{mid} (gray points, same data as Figure 1G). Cells are highlighted (maroon circles, 103 cells) if they were slowing-correlated during A_{mid} (see Results for definition).
(E) Lower bound of estimated density of slowing-correlated cells (see STAR Methods). Dashed lines indicate approximate boundaries of regions used to define reward-predictive cells (purple) and place cells that were stable across conditions (blue).
(F) Upper: average fluorescence activity of 142 slowing-correlated cells (6 mice, maroon trace) during A_{mid} blocks, and all spatially-modulated cells recorded simultaneously (6,935 cells, gray trace), plotted as a function of track position. Red line indicates A_{mid} reward location. As expected, slowing-correlated cells exhibited increased activity just prior to the reward (arrowhead). Lower: same averaging procedure applied to same cells, but during the interleaved A_{end} blocks from the same sessions. Red lines indicate reward location for A_{end} (solid) and, for comparison, A_{mid} (dashed). Bands indicate standard error of the mean. Despite some residual above-baseline fluorescence at the A_{mid} reward site (hollow arrowhead), the majority of slowing-correlated cell activity shifted to the A_{end} reward site (solid arrowhead), consistent with few if any place cells being slowing correlated.

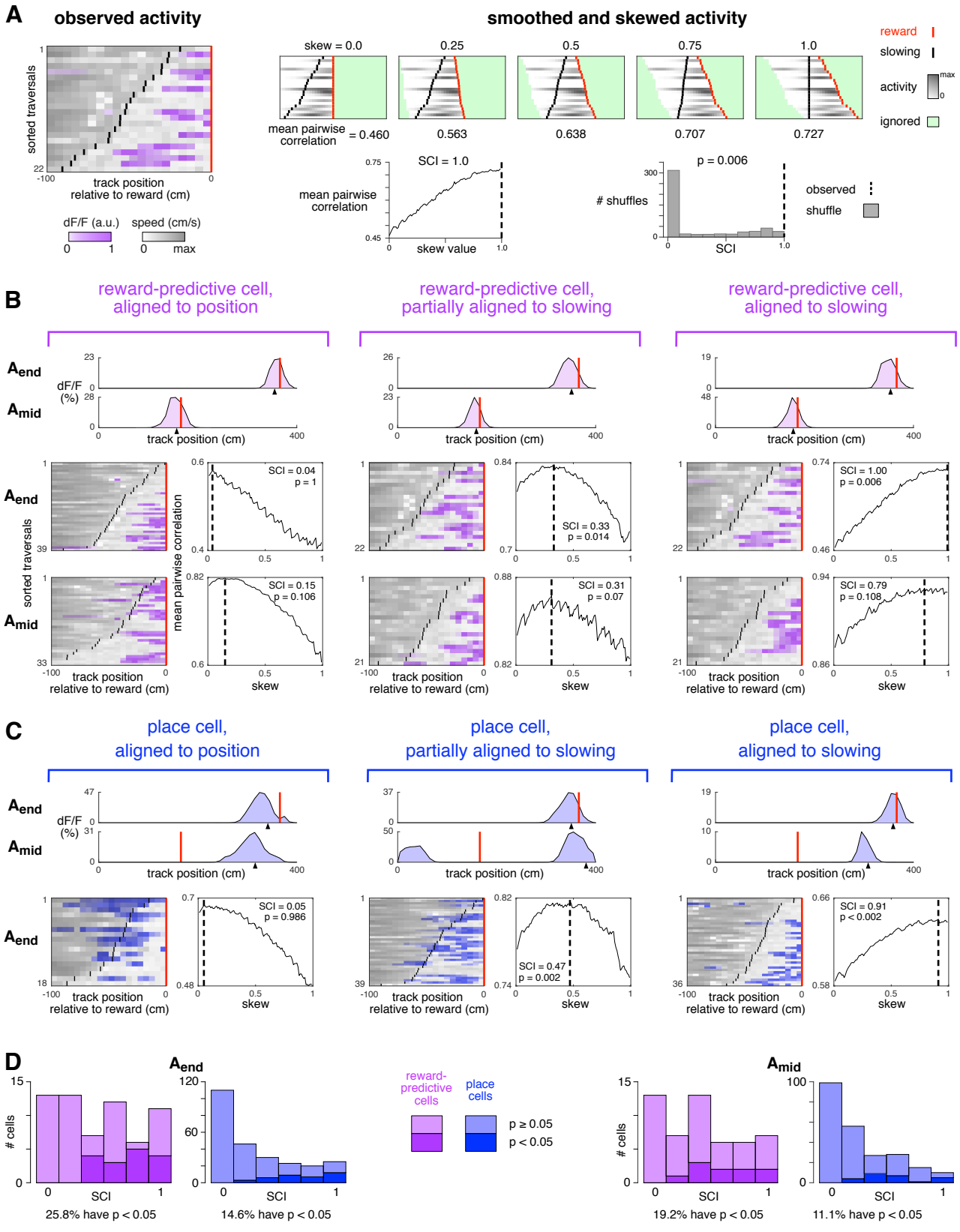
A
observed activity
smoothed and skewed activity
sorted traversals
track position
relative to reward (cm)
dF/F (a.u.)
speed (cm/s)
skew = 0.0
0.25
0.5
0.75
1.0
reward
slowing
activity
ignored
mean pairwise correlation = 0.460
0.563
0.638
0.707
0.727
SCI = 1.0
mean pairwise correlation
skew value
p = 0.006
# shuffles
observed
shuffle
SCI
B
reward-predictive cell, aligned to position
reward-predictive cell, partially aligned to slowing
reward-predictive cell, aligned to slowing
Aend
Amid
dF/F (%)
track position (cm)
sorted traversals
mean pairwise correlation
SCI = 0.04
p = 1
SCI = 0.33
p = 0.014
SCI = 1.00
p = 0.006
SCI = 0.15
p = 0.106
SCI = 0.31
p = 0.07
SCI = 0.79
p = 0.108
track position
relative to reward (cm)
skew
C
place cell, aligned to position
place cell, partially aligned to slowing
place cell, aligned to slowing
SCI = 0.05
p = 0.986
SCI = 0.47
p = 0.002
SCI = 0.91
p < 0.002
D
Aend
Amid
cells
SCI
reward-predictive cells
place cells
p ≥ 0.05
p < 0.05
25.8% have p < 0.05
14.6% have p < 0.05
19.2% have p < 0.05
11.1% have p < 0.05

Figure S4. The slowing correlation index (SCI) reveals that more reward-predictive cells than place cells were aligned with slowing, Related to STAR Methods and Figure 3.
(A) Illustration of how the SCI is computed for one cell. Observed activity (left panel) is taken in the 100 cm preceding reward (red line). Data is smoothed and skewed for many skew values ranging from 0 to 1 (upper panels, see STAR Methods). At each skew, the correlation is computed for every pair of trials and averaged over all pairs (lower middle panel). The skew that yielded the largest average correlation is taken as the SCI (dashed line). The observed SCI is compared to a shuffle distribution to yield a p-value (lower right panel).
(B) Examples of reward-predictive cells with various SCI values. Each cluster of panels corresponds to one cell. Upper panels: location of average activity, same conventions as Figure 1E. Lower left panels: locations of trial-by-trial slowing and activity for each context (A_{end} upper, A_{mid} lower), same conventions as left panel in A. Lower right panels: mean pairwise correlation vs skew, dashed line indicates observed SCI. Left cell: low and not significant SCI for both contexts. Middle cell: mid-range SCI, significantly aligned to slowing in context A_{end}. Right cell: high SCI significantly aligned to slowing in context A_{end}.
(C) Equivalent analysis and examples for place cells. Same conventions as in B.
(D) SCI values for all reward-predictive cells (purple) and reward-adjacent place cells (blue). Counts of cells with p-value less than 0.05 are indicated by darker colors. Counts are shown separately for A_{end} (left) and A_{mid} (right). Integrating data over both conditions, a greater fraction of reward-predictive cells than place cells had $p < 0.05$ (22.8% vs 12.9%), a statistically significant difference ($p = 0.012$, two-tailed Fisher's exact test).

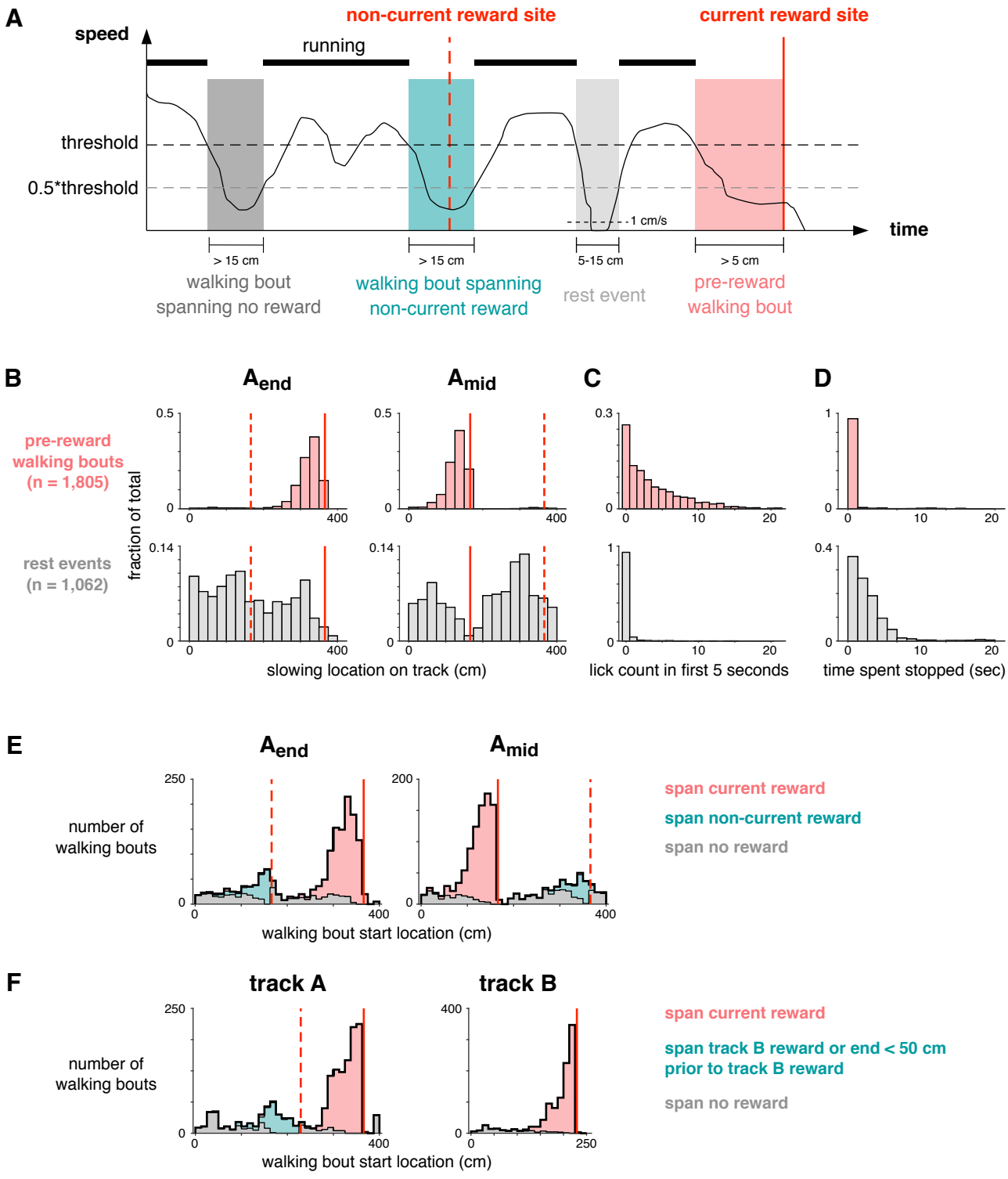
A
speed
running
non-current reward site
current reward site
threshold
0.5*threshold
1 cm/s
time
> 15 cm
> 15 cm
5-15 cm
> 5 cm
walking bout spanning no reward
walking bout spanning non-current reward
rest event
pre-reward walking bout
B
A_end
A_mid
C
D
pre-reward walking bouts (n = 1,805)
rest events (n = 1,062)
fraction of total
slowing location on track (cm)
lick count in first 5 seconds
time spent stopped (sec)
E
A_end
A_mid
number of walking bouts
walking bout start location (cm)
span current reward
span non-current reward
span no reward
F
track A
track B
number of walking bouts
walking bout start location (cm)
span current reward
span track B reward or end < 50 cm prior to track B reward
span no reward

Figure S5. Analysis of walking bouts and rest events, Related to STAR Methods and Figure 6.

(A) Schematic illustrating how movement speed (black trace) was used to define walking and rest events (colored patches). For detailed definitions, see STAR Methods.

(B-D) Rest events did not indicate anticipation of reward

(B) Locations where pre-reward walking bouts (top) or rest events (bottom) were initiated, plotted separately for blocks of A_{end} (left) or A_{mid} (right). To ensure mice were familiar with the structure of reward delivery and did not slow because they expected reward at other locations, data was only included from session 7 or later of training on condition $A_{end}A_{mid}$, and walking bouts from the first three traversals of each block were excluded.

(C) Number of licks during the first 5 seconds after the walking bout or rest event began.

(D) Overall duration in which mice were stopped (i.e. speed was slower than 1 cm/sec).

(E-F)Walking bouts occurred most frequently at the current reward site, but sometimes at the non-current reward site. The first three traversals of each block were excluded, and for condition $A_{end}A_{mid}$ data are only shown for session 7 or later.

(E) Starting locations for all walking bouts during condition $A_{end}A_{mid}$ (thick black trace), grouped by whether they spanned the current reward (pink), non-current reward (blue-green), or no reward (gray).

(F) Equivalent analysis for condition AB. Since the two rewards were delivered on different tracks, there was not an obvious definition of the "non-current reward location". Nevertheless, mice running on track A exhibited an increased frequency of slowing in the 150-200 cm range, presumably since this was close to 229 cm (location of track B reward). To ensure these walking bouts were considered related to the non-current reward location, the definition was expanded to include bouts that spanned any point in the 50 cm preceding 229 cm.

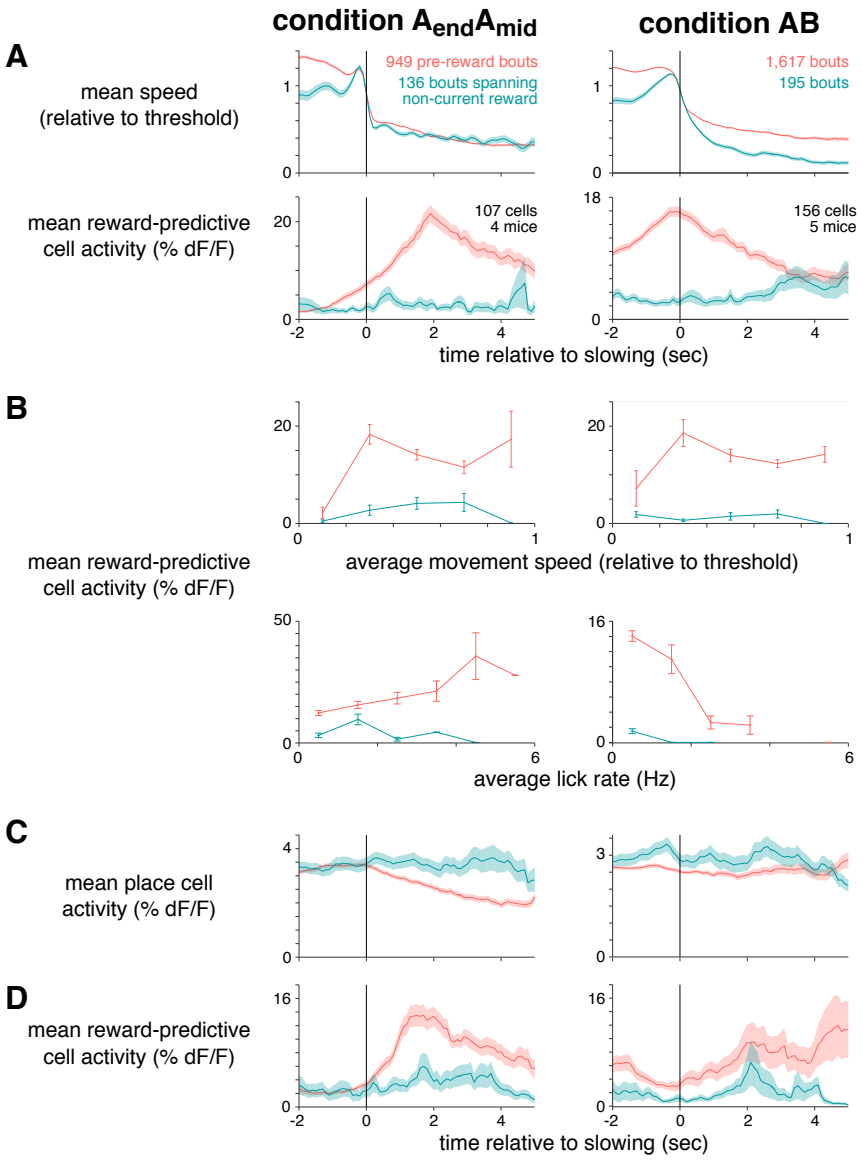
condition $A_{end}A_{mid}$
condition AB
A
mean speed
(relative to threshold)
949 pre-reward bouts
136 bouts spanning
non-current reward
1,617 bouts
195 bouts
mean reward-predictive
cell activity (% dF/F)
107 cells
4 mice
156 cells
5 mice
time relative to slowing (sec)
B
mean reward-predictive
cell activity (% dF/F)
average movement speed (relative to threshold)
average lick rate (Hz)
C
mean place cell
activity (% dF/F)
D
mean reward-predictive
cell activity (% dF/F)
time relative to slowing (sec)

Figure S6. Reward-predictive cells being more active during pre-reward walking bouts could not be explained by speed, licking, overall activity, or selection bias, Related to Figure 6.
(A-D) All plots compare activity or speed when mice walked before the current reward location (pink) or non-current reward location (blue-green). Error bars or bands indicate standard error of the mean when averaging across bouts. Activity of cells was first averaged within each bout, meaning error bars for activity overestimate the true uncertainty. For condition $A_{end}A_{mid}$, data are only shown for day 7 of training or later and the first three traversals of each block were excluded. Speed data only includes sessions in which reward-predictive cells were recorded.
(A) Mean speed (top) and reward-predictive cell activity (bottom) of slowing bouts as a function of time relative to slowing.
(B) Activity of reward-predictive cells when bouts were subdivided based on movement speed (top) or lick rate in the first 5 seconds after slowing (bottom).
(C) Activity of all cells that exhibited a spatially-modulated field in at least one context and were not classified as reward-predictive cells. Only includes sessions in which reward-predictive cells were also recorded. Though overall activity levels differed slightly between approaching current or non-current reward, they could not account for the difference in activity of reward-predictive cells.
(D) Activity of putative reward-predictive cells, analyzed to avoid selection bias (see STAR Methods). In condition $A_{end}A_{mid}$, activity was much greater when approaching the current reward, confirming that the effect shown in Figure 6 could not be attributed to selection bias. In condition AB, the putative reward-predictive cells might have included many place cells that were spuriously slowing-correlated on track B, and thus remapped randomly on track A, contributing a uniform positive offset in the pink trace.

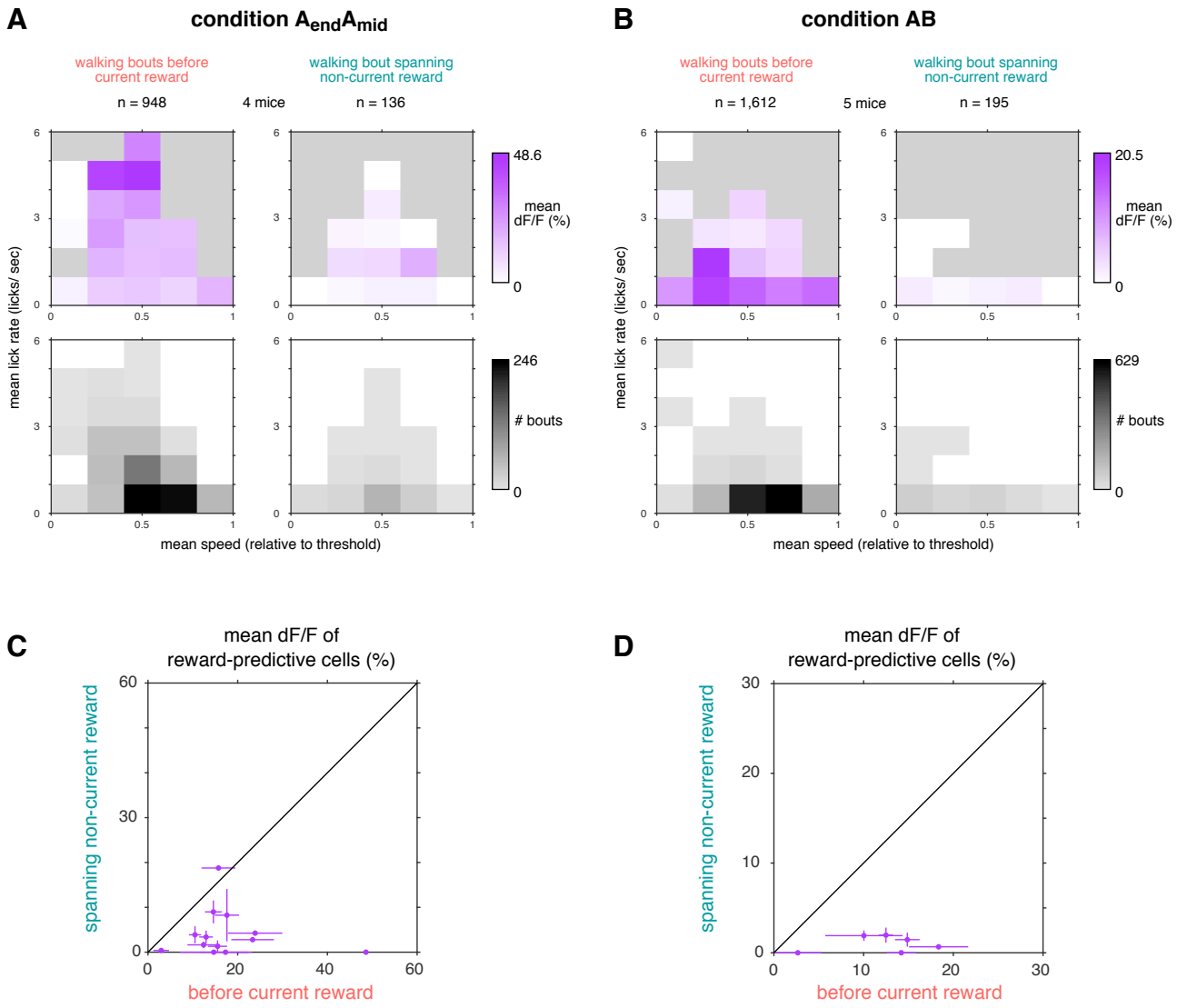
A
condition $A_{end}A_{mid}$
walking bouts before current reward
walking bout spanning non-current reward
n = 948
4 mice
n = 136
48.6
mean dF/F (%)
0
246
bouts
0
mean lick rate (licks/ sec)
mean speed (relative to threshold)
B
condition AB
walking bouts before current reward
walking bout spanning non-current reward
n = 1,612
5 mice
n = 195
20.5
mean dF/F (%)
0
629
bouts
0
mean lick rate (licks/ sec)
mean speed (relative to threshold)
C
mean dF/F of reward-predictive cells (%)
spanning non-current reward
before current reward
D
mean dF/F of reward-predictive cells (%)
spanning non-current reward
before current reward

Figure S7. Reward-predictive cells being more active during pre-reward walking bouts could not be explained by the conjunction of speed and lick rate, Related to Figure 6.
(A) Each bout was categorized based on the average lick rate (y-axis) and average speed (x-axis) in the first 5 seconds. Top panels: Average reward-predictive cell activity during bouts in each category. Bottom panels: number of bouts in each category. Separate plots are shown for pre-reward walking bouts (left) and walking bouts spanning the non-current reward (right). Data are only shown for day 7 of training or later and the first three traversals of each block were excluded.
(B) Equivalent analysis for condition AB, except that all training days and traversals were included.
(C) Scatter plot of reward predictive-cell activity during pre-reward walking bouts (x-axis) and walking bouts spanning the non-current reward (y-axis). Error bars indicate standard error of the mean. Each point is the average of bouts from one category (i.e. a single bin from panel A), allowing a direct comparison of reward-predictive cell activity when controlling for the conjunction of lick rate and walking speed. In nearly every case, activity was greater when walking before the current reward than the non-current reward, confirming the result of Figure 6.
(D) Equivalent analysis of data in panel B.